OsteoArthritis and Cartilage (2007) **15,** 35–47

doi:10.1016/j.joca.2006.06.005

Osteoarthritis and Cartilage

ICRS International Cartilage Repair Society

OARSI OSTEOARTHRITIS RESEARCH SOCIETY INTERNATIONAL

Effect of synovial fluid on boundary lubrication of articular cartilage

T. A. Schmidt Ph.D.* and R. L. Sah M.D., Sc.D.

Department of Bioengineering and Whitaker Institute of Biomedical Engineering, University of California – San Diego, La Jolla, CA, USA

Summary

Objectives: The lubrication of articulating cartilage surfaces in joints occurs through several distinct modes. In the boundary mode of lubrication, load is supported by surface-to-surface contact, a feature that makes this mode particularly important for maintenance of the normally pristine articular surface. A boundary mode of lubrication is indicated by a kinetic friction coefficient being invariant with factors that influence formation of a fluid film, including sliding velocity and axial load. The objectives of this study were to (1) implement and extend an *in vitro* articular cartilage-on-cartilage lubrication test to elucidate the dependence of the friction properties on sliding velocity, axial load, and time, and establish conditions where a boundary mode of lubrication is dominant, and (2) determine the effects of synovial fluid (SF) on boundary lubrication using this test.

Methods: Fresh bovine osteochondral samples were analyzed in an annulus-on-disk rotational configuration, maintaining apposed articular surfaces in contact, to determine static (μ_{static} and $\mu_{\text{static},N_{\text{eq}}}$) and kinetic ($\langle\mu_{\text{kinetic}}\rangle$ and $\langle\mu_{\text{kinetic},N_{\text{eq}}}\rangle$) friction coefficients, each normalized to the instantaneous and equilibrium (N_{eq}) normal loads, respectively.

Results: With increasing pre-sliding durations, μ_{static} and $\mu_{\text{static},N_{\text{eq}}}$ were similar, and increased up to 0.43 ± 0.03 in phosphate buffered saline (PBS) and 0.19 ± 0.01 in SF, whereas $\langle\mu_{\text{kinetic}}\rangle$ and $\langle\mu_{\text{kinetic},N_{\text{eq}}}\rangle$ were steady. Over a range of sliding velocities of 0.1–1 mm/s and compression levels of 18% and 24%, $\langle\mu_{\text{kinetic}}\rangle$ was 0.072 ± 0.010 in PBS and 0.014 ± 0.003 in SF, and $\langle\mu_{\text{kinetic},N_{\text{eq}}}\rangle$ was 0.093 ± 0.005 in PBS and 0.018 ± 0.002 in SF.

Conclusions: A boundary mode of lubrication was achieved in a cartilage-on-cartilage test configuration. SF functioned as an effective friction-lowering boundary lubricant for native articular cartilage surfaces.

Key words: Boundary lubrication, Articular cartilage, Synovial fluid, Biomechanics.

Introduction

Articular cartilage normally serves as the low friction, wear resistant, load bearing tissue at the end of long bones in skeletal joints[1]. The articulation of cartilage against cartilage presents a major biomechanical challenge, with an individual typically taking 1–4 million steps each year[2]. Unfortunately, the pristine structure of the articular cartilage surface often deteriorates with aging and arthritis, becoming increasingly roughened and eroded, with development of pain and dysfunction, and progressing to osteoarthritis[3]. Thus, the extent and modes of the normal lubrication of articulating cartilage surfaces are important to understand.

A number of physicochemical modes of lubrication occur in synovial joints and have been classified as fluid film or boundary[4,5]. The operative lubrication modes depend on the normal and tangential forces on the articulating tissues, on the relative rate of tangential motion between these surfaces, and on the time history of both loading and motion[6,7]. The friction coefficient, μ, provides a quantitative measure, and is defined as the ratio of tangential friction force to the normal force. One type of fluid-mediated lubrication mode is hydrostatic. At the onset of loading and typically for a prolonged duration, the interstitial fluid within cartilage becomes pressurized, due to the biphasic nature of the tissue; fluid may also be forced into the asperities between articular surfaces through a weeping mechanism[8]. Pressurized interstitial fluid and trapped lubricant pools may therefore contribute significantly to the bearing of normal load with little resistance to shear force, facilitating a very low μ[4]. Also, at the onset of loading and/or motion, squeeze film, hydrodynamic, and elastohydrodynamic types of fluid film lubrication occur, with pressurization, motion, and deformation acting to drive viscous lubricant from and/or through the gap between two surfaces in relative motion.

In contrast, in boundary lubrication, load is supported by surface-to-surface contact, and the associated frictional properties are determined by lubricant surface molecules. This mode has been proposed to be important because the apposing cartilage layers make contact over ~10% of the total area, and this may be where most of the friction occurs[9]. Furthermore, with increasing loading time and dissipation of hydrostatic pressure, lubricant-coated surfaces bear an increasingly higher portion of the load relative to pressurized fluid, and consequently, μ can become increasingly dominated by this mode of lubrication[8,10]. A boundary mode of lubrication is indicated by values of μ during steady sliding being invariant with factors that influence formation of a fluid film, such as relative sliding velocity and axial load[11]. Boundary lubrication, in essence, mitigates stick-slip[10], and is therefore manifest as decreased resistance

*Address correspondence and reprint requests to: Robert L. Sah, M.D., Sc.D., Department of Bioengineering, Mail Code 0412, 9500 Gilman Drive, University of California – San Diego, La Jolla, CA 92093-0412, USA. Tel: 1-858-534-0821; Fax: 1-858-822-1614; E-mail: rsah@ucsd.edu
Received 28 September 2005; revision accepted 5 June 2006.

both to steady motion and the start-up of motion. The latter situation is relevant to load bearing articulating surfaces after prolonged compressive loading (e.g., sitting or standing *in vivo*)[12]. Typical wear patterns of cartilage surfaces[13] also suggest that boundary lubrication of articular cartilage is critical to the protection and maintenance of the articular surface structure.

A variety of time-dependent *in vitro* mechanical tests have been developed to assess the effectiveness and modes of articular cartilage lubrication. Since joints are subject to sequential periods of rest and motion, the transition to motion represents one lubrication challenge, and steady-state motion represents an additional lubrication challenge. Analogously, friction coefficients can be measured at start-up from a static condition, i.e., μ_{static}, or under steady sliding or kinetic conditions, $\mu_{kinetic}$, although most tests have focused on the latter (Table I). μ_{static} increases (e.g., from $\sim$0.02–0.25) with increasing loading times (5 s–45 min) for both cartilage–cartilage and cartilage–metal interfaces[6]. $\mu_{kinetic}$ is low ($\sim$0.001–0.05) at early times after loading where fluid pressurization is significant, for normal articulating cartilage surfaces[14–16]. Conversely, when fluid depressurization is allowed after compression of apposed articular surfaces[16], as well as between cartilage and glass[17,18], $\mu_{kinetic}$ is higher ($\sim$0.1–0.6). $\mu_{kinetic}$ also depends on the rotational velocity with cartilage apposed to and rotated against steel[19].

Cartilage-on-cartilage lubrication tests provide a configuration mimicking certain aspects of naturally articulating surfaces. Lubrication tests of cartilage against artificial surfaces may reproduce some, but not all, of the molecular interactions that are operative in physiological articulation[20]. The $\mu_{kinetic}$ of cartilage against an artificial surface can vary significantly (e.g., 0.14 for polystyrene[18] vs 0.28 for glass[17]), suggesting that the surface apposing the articular cartilage is an important determinant of friction. Cartilage-on-cartilage tests may be performed in a sliding or rotational configuration, resulting in areas of contact between surfaces under relative motion; such contact areas may be either moving or constant, respectively. While the sliding test configuration models certain aspects of physiological kinematics[21], the rotational configuration has advantages for examining putative boundary lubricants of articular cartilage at a like interface[16]. In the sliding configuration, with a moving contact area, both fluid film and boundary lubrication are generally operative due to fluid pressurization and exudation, even at relatively slow sliding velocities[22,23]. In the rotational configuration, ploughing friction losses are minimized because the apposed surfaces remain in contact[24], and fluid pressure effects are minimal at relatively slow velocities after the initial pressure dissipates. Furthermore, with the use of an annular geometry[16,25,26], the variation in sliding velocity is reduced (due to its proportionality to the radius), as is the time required for fluid depressurization. Using this annulus-on-disk configuration for a cartilage–cartilage interface with nasal septal cartilage, Davis *et al.* showed that synovial fluid (SF) lubricated better than Gey's balanced salt solution[25]. With articular cartilage samples, Malcom and Fung also found that SF lubricated static and dynamically loaded samples, after step loading and partial fluid depressurization, better than phosphate buffered saline (PBS)[16,26]. Thus, the annulus-on-disk rotational test configuration appears to be advantageous for studying boundary lubrication at an articular cartilage-on-cartilage interface, possibly modulated by SF.

The objectives of this study were to (1) implement and extend an *in vitro* articular cartilage-on-cartilage annulus-on-disk lubrication test to elucidate the dependence of the friction properties on sliding velocity, axial load, and time, and establish conditions where a boundary mode of lubrication is dominant, and (2) determine the effects of SF on boundary lubrication using this test.

Table I
Symbols used for variables and parameters

Variable or parameter	Symbol
Stretch ratio	Λ_z
Kinetic friction coefficient	$\mu_{kinetic}$
Kinetic friction coefficient normalized by equilibrium axial load	$\langle\mu_{kinetic,N_{eq}}\rangle$
Static friction coefficient	μ_{static}
Static friction coefficient normalized by equilibrium axial load	$\mu_{static,N_{eq}}$
Axial load	N
Equilibrium axial load	N_{eq}
Effective radius	R_{eff}
Inner radius	R_i
Outer radius	R_o
Normal stress	σ
Equilibrium normal stress	σ_{eq}
Peak normal stress	σ_{peak}
Axial torque	τ
Time	t
Pre-sliding duration	T_{ps}
Stress relaxation duration	T_{sr}
Effective sliding velocity	v_{eff}

Methods

MATERIALS

Skeletally mature adult bovine stifle joints (1–2 years old) were obtained as described previously[27]. Bovine SF was aspirated from synovial joints within 10–15 min of slaughter, visually inspected to ensure no blood contamination, then aliquoted and stored at −80°C for several months before use.

SAMPLE PREPARATION

Osteochondral samples were prepared from the patellofemoral groove from four joints [Fig. 1(A)], in a manner similar to that described previously[28]. Osteochondral blocks were isolated first, and then osteochondral samples ($n = 16$) were cut from the blocks using a low speed drill press with custom stainless steel coring bits, using PBS at 4°C for irrigation. Each sample consisted of an osteochondral core, radius = 6 mm, and an apposed osteochondral annulus (outer radius, $R_o = 3.2$ mm, and inner radius, $R_i = 1.5$ mm), both with central holes (radius = 0.5 mm) drilled down into and exiting the bone to facilitate fluid depressurization [Fig. 1(B)]. (Pilot studies indicated that inclusion of these holes reduced the time to attain 50% stress relaxation by $\sim$10%.) The cartilage thickness of each core and annulus were then measured with digital calipers at four equally spaced locations around the circumferences and averaged, and the overall cartilage thickness was taken as the sum of the two average thicknesses (3.32 ± 0.30 mm, mean ± SD for all 16 samples). Samples were used without prior freezing to preserve lubrication properties[16], and bathed in test lubricant, completely immersing

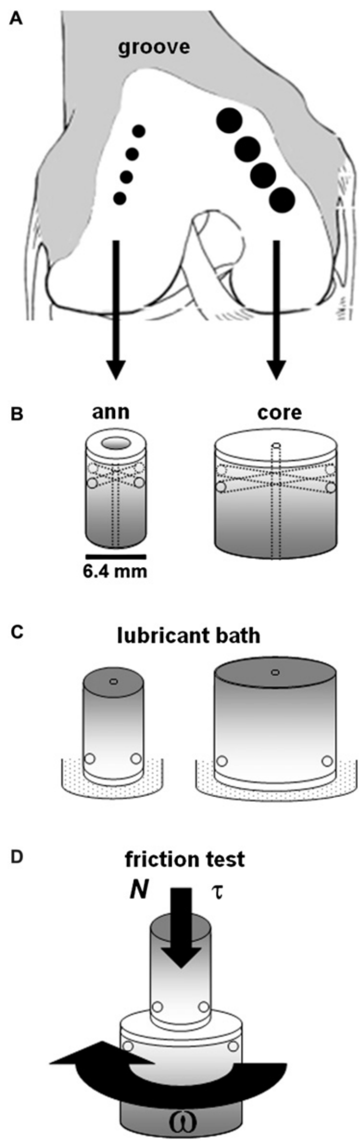

Fig. 1. Diagram of harvest location, specimen preparation and lubricant bath incubation, and friction testing. Blocks were harvested from the patellofemoral groove of mature bovine stifle joints (A) from which osteochondral annulus (ann) and core sample (B) were prepared. Sample pairs were incubated in the test bath solution (PBS or SF) at 4°C for 24–48 h (C) prior to friction testing (D).

the cartilage [Fig. 1(C)], at 4°C for 24–48 h prior to lubrication testing.

LUBRICATION TEST SETUP

For lubrication testing, the sample core and annulus were placed in apposition, compressed axially, and subjected to relative rotation. Samples were tested in an ELF 3200 (Bose EnduraTEC, Minnetonka, MN) with custom sample fixtures, axial and rotational actuators, an internal sensor for axial displacement (±6.250 mm range), and sensors for axial load (N) and torque (τ) (with ranges of ±45.0 N, and ±70.0 N mm, respectively). Samples were brought to room temperature, then placed concentrically in the ELF 3200, with the core on the rotational actuator below, and the annulus on the sensors and axial actuator above [Fig. 1(D)]. A test lubricant reservoir was formed by circumferentially securing an inert silicon rubber tube around the core and adding ~0.5 ml of test lubricant, completely immersing both cartilage test surfaces. The samples were then brought into contact, defined as the axial position half-way between the points of initial and final contact, determined as the positions of maximum and minimum N, respectively, measured during one complete revolution. The sample surfaces were aligned normal to the rotation axis, as judged by the axial distance between the points of initial and final contacts being <0.1 mm (i.e., <4% of the thickness of the apposed articular cartilage). During rotational testing, the change in radial distance between the outer edge of the core and annulus cartilage surfaces was estimated to be 0.0–0.5 mm. Even with the highest value, the contact area during rotation was calculated to change by only ~13%, indicating that the contacting areas were approximately constant.

EXPERIMENTAL DESIGN

To determine the test conditions in which boundary lubrication was the dominant mode at the articular cartilage-on-cartilage interface, the dependence of frictional properties on post-compression pause durations, compression level, and sliding velocity was examined. Specifically, the effects of stress relaxation duration (T_{sr}, the duration allowed for fluid depressurization after the sample is compressed), compression ($1-\Lambda_Z$, where Λ_Z is the stretch ratio[26]), effective sliding velocity ($v_{eff}=\omega R_{eff}$, where ω is the angular frequency, in rad/s, and R_{eff} is the effective radius calculated to be $2/3[(R_o^3-R_i^3)/(R_o^2-R_i^2)]=2.4$ mm by integrating the shear stress distribution over the annular contact area[16]), and pre-sliding duration (T_{ps}, the duration the sample is stationary prior to rotation), on the lubrication properties of articular cartilage were assessed with PBS, and then SF, as lubricant solutions (Fig. 2). Samples were first bathed in a small volume (~1 ml) of PBS, and then tested for lubrication properties in PBS. Samples were subsequently bathed in SF, followed by lubrication testing in SF. Due to the potential structural, and therefore functional, alterations of lubricant molecules within SF, protease inhibitors were not included in the test lubricants. Control studies indicated no deterioration of friction properties over the duration of the test period, as friction coefficients (described below) of samples, stored at 4°C, tested in SF (at $1-\Lambda_Z=18\%$ and 24%, with $T_{sr}=60$ min, $v_{eff}=0.3$ mm/s, and $T_{ps}=120$ s) on day 4 were similar to those measured on day 1 ($97\pm8\%$ for μ_{static} and $88\pm9\%$ for $\langle\mu_{kinetic}\rangle$, $n=4$). Preliminary tests also confirmed that testing in PBS then SF did not affect measured values in SF. Mechanical properties appeared to be maintained as well since equilibrium N values (N_{eq}) attained in the second test lubricant were within ~6% of the first. Data were collected at 20 Hz during the $v_{eff}=3$ mm/s test revolutions, and 10 Hz for all others.

Effect of stress relaxation

Samples ($n=4$) were compressed at a constant rate of 0.002 mm/s to $1-\Lambda_Z=18\%$ of the total cartilage thickness [Fig. 2(A)], then tested by rotating +2 revolutions, immediately followed by −2 reset revolutions at $v_{eff}=0.3$ mm/s (which is on the order of that used in other test configurations[29] and has been found to maintain a boundary or mixed

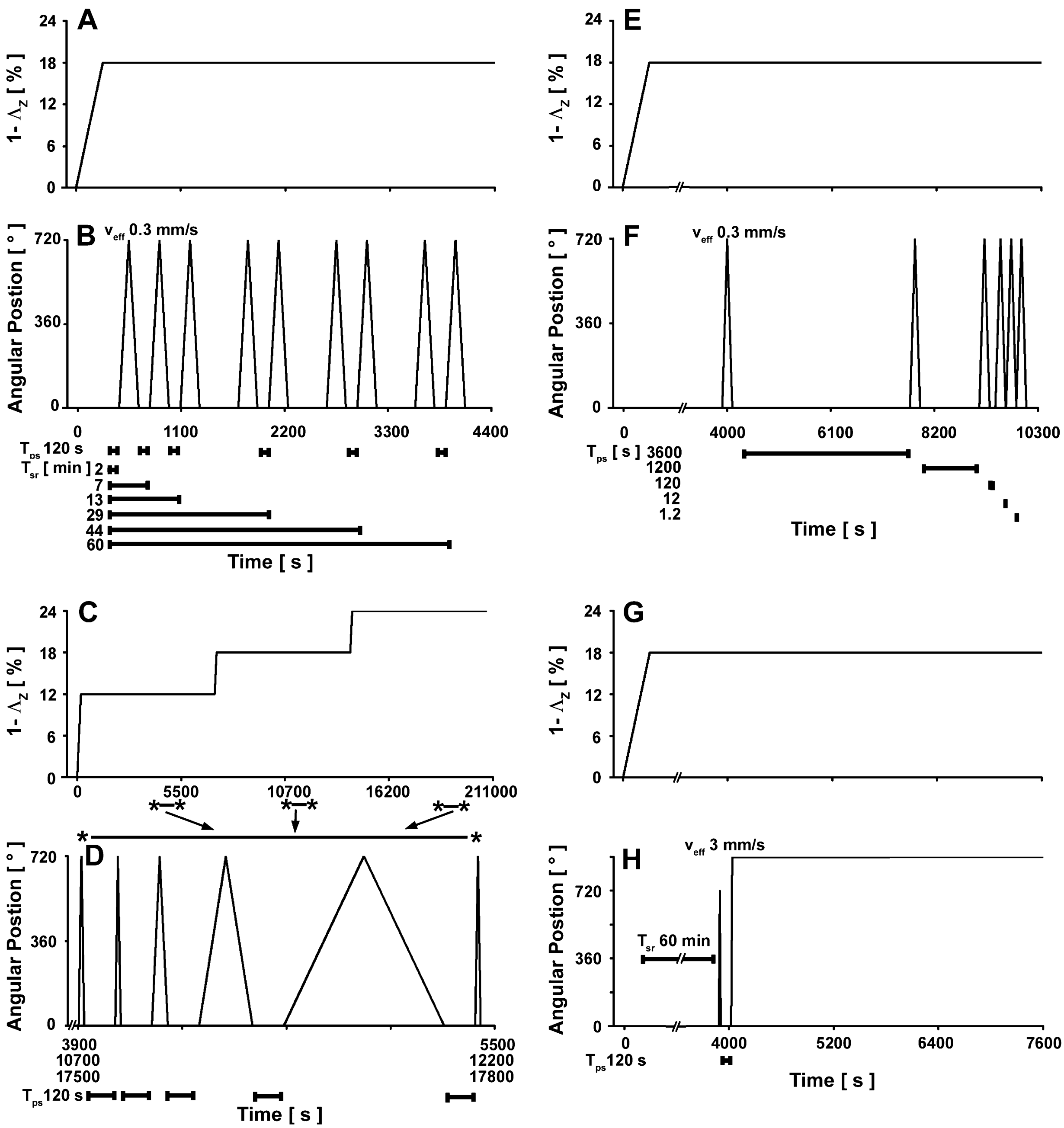

Fig. 2. Lubrication test protocols defined by stress relaxation duration (T_{sr}), compression ($1-\Lambda_Z$), effective sliding velocity (v_{eff}), and presliding duration (T_{ps}). Samples were compressed axially by $1-\Lambda_Z = 18\%$ (A, E, and G), or 12%, 18%, and 24% (C) of the total cartilage thickness. Rotational test protocols were then respectively used to determine the effects of T_{sr} (B), $1-\Lambda_Z$ and v_{eff} (D), T_{ps} (F), and fluid depressurization (H) on the lubrication properties of articular cartilage for PBS and/or SF lubricants. Schematics (B, D, and F), only show + test revolution sequence, as the identical − test sequence proceeded subsequently with revolutions in the opposite direction.

mode of lubrication[19]). Test revolutions were then performed at $T_{sr} = 2$, 7, 13, 29, 44, and 60 min, with $T_{ps} = 120$ s between each [Fig. 2(B)]. The 60 min duration was based on a characteristic time constant $t_{char} = l^2/(H_A k_p)$, where l is the characteristic length, $(R_o - R_i)/2$ mm $= 0.85$ mm, H_A is the modulus, 0.31 MPa, and k_p is the hydraulic permeability, 10^{-15} m^2/Pa s[27,30,31], yielding $t_{char} = 45$ min, as validated experimentally, below. Pilot studies indicated $T_{ps} = 120$ s was sufficient to measure differences between μ_{static} and $\langle\mu_{kinetic}\rangle$, defined below, such that the stick-slip process mitigated by boundary lubrication could be observed. Samples were then unloaded and held at $1-\Lambda_Z = 0\%$ for 120 min to allow for creep. Samples were then compressed to $1-\Lambda_Z = 18\%$ again, and the test sequence was then repeated in the opposite direction of rotation.

Effect of sliding velocity and compression

Samples ($n = 4$) were compressed to $1-\Lambda_Z = 12\%$ of the total cartilage thickness [Fig. 2(C)], as described above, and allowed $T_{sr} = 60$ min for stress relaxation and fluid depressurization. The test sequence was initiated by conditioning the sample by rotating +2 revolutions and reset with −2 revolutions at $v_{eff} = 3$ mm/s. Samples were then tested by rotating +2 revolutions, immediately followed by −2 reset revolutions at v_{eff} of 3, 1, 0.3, 0.1, and then 3 mm/s, with $T_{ps} = 120$ s between each v_{eff} [Fig. 2(D)]. The test sequence was then repeated in the opposite direction of rotation. Samples were subsequently compressed at the same rate (0.002 mm/s) to $1 - \Lambda_Z = 18\%$ and then 24% of the total cartilage thickness and the entire test sequence was repeated at each compression level in both directions of rotation.

Effect of pre-sliding duration

Samples ($n = 4$) were compressed to $1 - \Lambda_Z = 18\%$ of the total cartilage thickness at 0.002 mm/s [Fig. 2(E)] and allowed to stress relax as described above. The test sequence was initiated in a similar manner as well, except with $v_{eff} = 0.3$ mm/s. The samples were then tested by rotating +2 revolutions, immediately followed by −2 reset revolutions with $v_{eff} = 0.3$ mm/s and $T_{ps} = 3600$, 1200, 120, 12, and 1.2 s [Fig. 2(F)]. The test sequence was then repeated with rotation in the opposite direction.

Role of fluid depressurization during rotation

With SF as the test lubricant, samples ($n = 4$) were compressed to $1 - \Lambda_Z = 18\%$ of the total cartilage thickness [Fig. 2(G)], and allowed to stress relax as described above. The test sequence was initiated as described above, with $v_{eff} = 3$ mm/s. After $T_{ps} = 120$ s, samples were then subjected to +2.5 revolutions with $v_{eff} = 3$ mm/s, and finally monitored for another 60 min, to assess possible stress relaxation, indicative of fluid depressurization [Fig. 2(H)].

DATA ANALYSIS

To evaluate the lubrication properties of the articular cartilage in test lubricants (PBS and SF), four friction coefficients (μ) of the form $\mu = \tau/(R_{eff}N)$ were calculated, where τ is torque, N is axial load, and R_{eff} is effective radius, described above. Classical static (μ_{static}) and kinetic ($\langle\mu_{kinetic}\rangle$) friction coefficients were calculated from the instantaneous μ described above. μ_{static} was calculated as the peak value of μ, just after (within 10°) the start of rotation, and $\langle\mu_{kinetic}\rangle$ was calculated from μ averaged during the second complete revolution of the test sample. Another static friction coefficient, $\mu_{static,N_{eq}}$, was calculated using the peak $|\tau|$, also measured within 10° of the start of rotation, and the axial load at the end of the 60 min stress relaxation period, N_{eq}. In all of the above tests except the first (which examined the effect of stress relaxation), another kinetic friction coefficient, $\langle\mu_{kinetic,N_{eq}}\rangle$, was calculated using the $|\tau|$ averaged during the second complete revolution of the test sample, and N_{eq}. The values of μ_{static}, $\mu_{static,N_{eq}}$, $\langle\mu_{kinetic}\rangle$, and $\langle\mu_{kinetic,N_{eq}}\rangle$ were then averaged for the + and − revolutions in each test to account for potential directional effects on τ measurements. The normal stress (σ), in units of MPa, was calculated as $|N|/(\pi[R_o^2 - R_i^2])$. The equilibrium stress values (σ_{eq}) were calculated after $T_{sr} = 60$ min; the peak stress (σ_{peak}) values were calculated from the peak $|N|$ during rotation, and averaged for the + and − revolutions.

Data are presented as the mean ± S.E.M. Repeated measures analysis of variance (ANOVA) was used to assess the effect of test lubricant, T_{sr}, $1 - \Lambda_Z$, v_{eff}, and T_{ps} on μ_{static}, $\mu_{static,N_{eq}}$, $\langle\mu_{kinetic}\rangle$, and $\langle\mu_{kinetic,N_{eq}}\rangle$. Where there were three factors, and test lubricant had a significant effect, data for each lubricant were analyzed further using a two-factor ANOVA. Statistical analysis was implemented with Systat 10.2 (Systat Software, Inc., Richmond, CA).

Results

LUBRICATION TEST CHARACTERIZATION

The sample preparation and lubrication test setup enabled precise measurements of τ and N during the various tests. Typical $|\tau|$ values ranged from 0.1 to 5 N mm, with transient torque values immediately after the start of the test revolution (corresponding to μ_{static} and $\mu_{static,N_{eq}}$) being clearly distinguishable (with the torque sensor precision of ±0.01 N mm) from the steady-state values by the beginning of the second test revolution. Typical $|N|$ values ranged from 1 to 10 N during the test, which were clearly resolved by the axial load sensor (precision of ±0.1 N) with feedback control of the axial displacement (precision of ±0.001 mm). Only the raw data from the +2 revolutions of the tests are shown subsequently, for brevity, since reduction of data from the −2 revolutions of the tests gave friction coefficients that were similar on average (within 1 ± 14%, mean ± SD) to those determined from the +2 revolutions.

EFFECT OF STRESS RELAXATION

The $|\tau|$ [Fig. 3(A,B)] and $|N|$ [Fig. 3(C,D)] during the 2 test revolutions varied with T_{sr}. In both the PBS and SF test lubricants, $|\tau|$ and $|N|$ decreased qualitatively as T_{sr} increased from 2 to 7 min. $|\tau|$ was greater in PBS than SF, while $|N|$ was similar in PBS and SF. The peak $|\tau|$ [see insets of Fig. 3(A,B)] dissipated to relatively steady values by 360°. The $|N|$ was cyclical during the 2 test revolutions, peaking at approximately 180° and 540°, with the amplitude being greater at 180° compared to 540°. The σ_{peak} values attained at $1 - \Lambda_Z = 18\%$ in PBS and SF ranged (for $T_{sr} = 60$–2 min) from 0.42 ± 0.05 to 0.21 ± 0.03 MPa and 0.46 ± 0.06 to 0.23 ± 0.03 MPa, respectively. The σ_{eq} values attained at $T_{sr} = 60$ min and $1 - \Lambda_Z = 18\%$ in PBS and SF were both 0.10 ± 0.01 MPa.

Friction was modulated by test lubricant and T_{sr} (Fig. 4). μ_{static} varied with test lubricant (being higher in PBS than SF, $P < 0.05$) and T_{sr} ($P < 0.001$), with an interaction effect ($P < 0.001$) [Fig. 4(A)]. In PBS, μ_{static} increased with T_{sr} and ranged from 0.18 to 0.25. In SF, μ_{static} averaged 0.11. Similarly, $\mu_{static,N_{eq}}$ varied with test lubricant (also being higher in PBS than SF, $P < 0.05$) and T_{sr} ($P < 0.001$), without an interaction effect ($P = 0.06$) [Fig. 4(B)]. However, contrary to μ_{static}, $\mu_{static,N_{eq}}$ decreased with increasing T_{sr}, and ranged from 0.37 to 0.28 in PBS, and 0.21 to 0.11 in SF. Nevertheless, in both PBS and SF, μ_{static} and $\mu_{static,N_{eq}}$ converged to a similar value as $T_{sr} \to 60$ min. Thus, in the subsequent tests where $T_{sr} = 60$ min, only $\mu_{static,N_{eq}}$ values are reported since μ_{static} values were similar (on average within 5 ± 19%, mean ± SD), due to $|N_{eq}|$ being similar to $|N|$ immediately after the start of rotation. Lastly, $\langle\mu_{kinetic}\rangle$ varied with T_{sr} ($P < 0.001$), with an interaction effect ($P < 0.001$) and without an effect of test lubricant ($P = 0.07$) [Fig. 4(C)]. $\langle\mu_{kinetic}\rangle$ increased slightly with T_{sr} and was greater in PBS than SF, ranging from 0.065 to 0.096 in PBS, and 0.029 to 0.035 in SF.

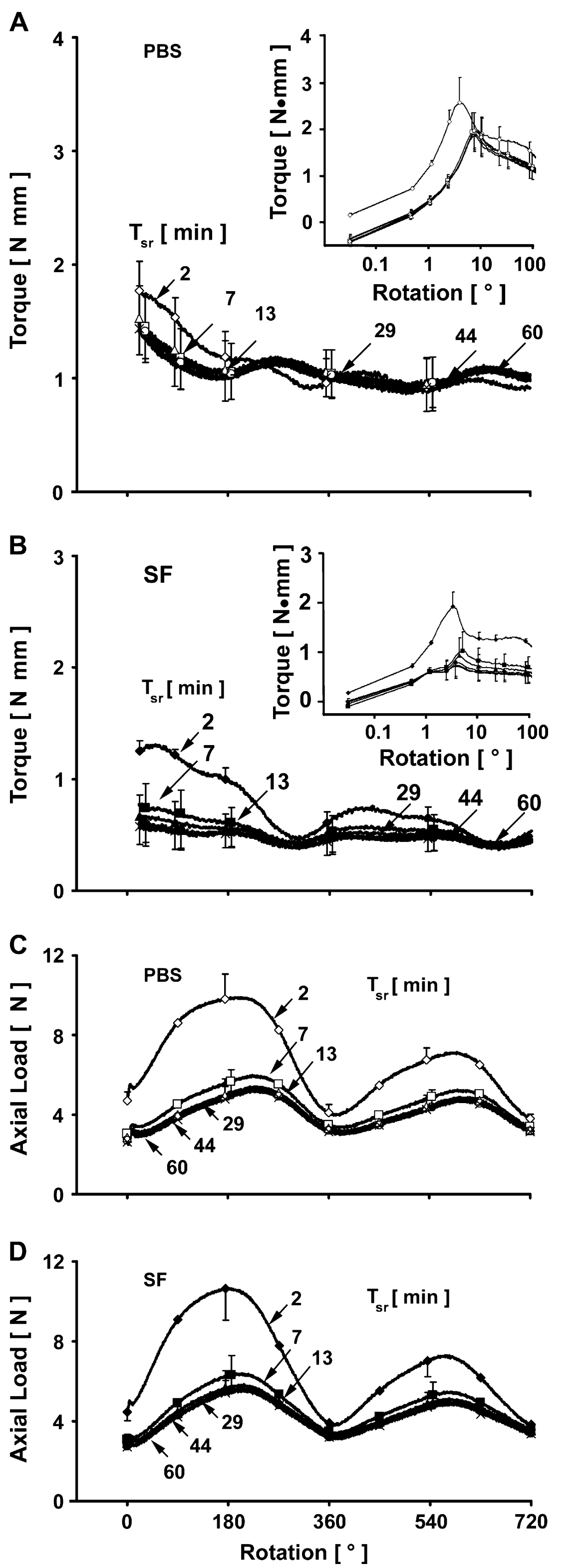

Fig. 3. Torque (A, B with log scale insets to show values at small rotation angles) and axial load (C and D) measurements vs rotation in test baths of PBS and SF at 18% compression ($1 - \Lambda_Z$) after 2, 7, 13, 29, 44, and 60 min stress relaxation duration (T_{sr}), at an effective sliding velocity (v_{eff}) of 0.3 mm/s with a 120 s pre-sliding duration (T_{ps}). Mean ± S.E.M., $n = 4$.

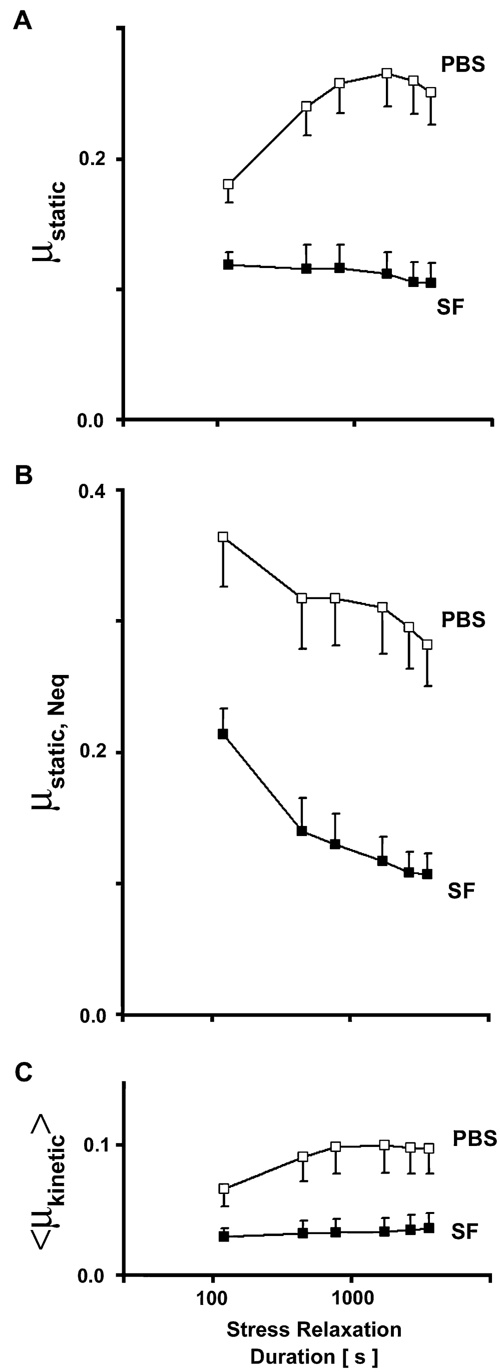

Fig. 4. Static, μ_{static} (A), $\mu_{static,N_{eq}}$ (B), and kinetic, $\langle\mu_{kinetic}\rangle$ (C) friction coefficients in PBS and SF at 18% compression ($1 - \Lambda_Z$) after 2, 7, 13, 29, 44, and 60 min stress relaxation duration (T_{sr}), at an effective sliding velocity (v_{eff}) of 0.3 mm/s with a 120 s pre-sliding duration (T_{ps}). Mean ± S.E.M., $n = 4$.

EFFECT OF SLIDING VELOCITY AND COMPRESSION

The $|\tau|$ [Fig. 5(A,B)] and $|N|$ [Fig. 5(C,D)] during the 2 test revolutions at $1 - \Lambda_Z = 18\%$ varied with v_{eff}. In both the PBS and SF test lubricants, $|\tau|$ and $|N|$ increased qualitatively with v_{eff}. $|\tau|$ was greater in PBS than SF, while $|N|$ was similar in PBS and SF. The peak $|\tau|$ [see insets of Fig. 5(A,B)] dissipated to an approximately steady-state value by 360°, as indicated by the ratio of $\tau_{360-720°}$ to $\tau_{360°}$ being

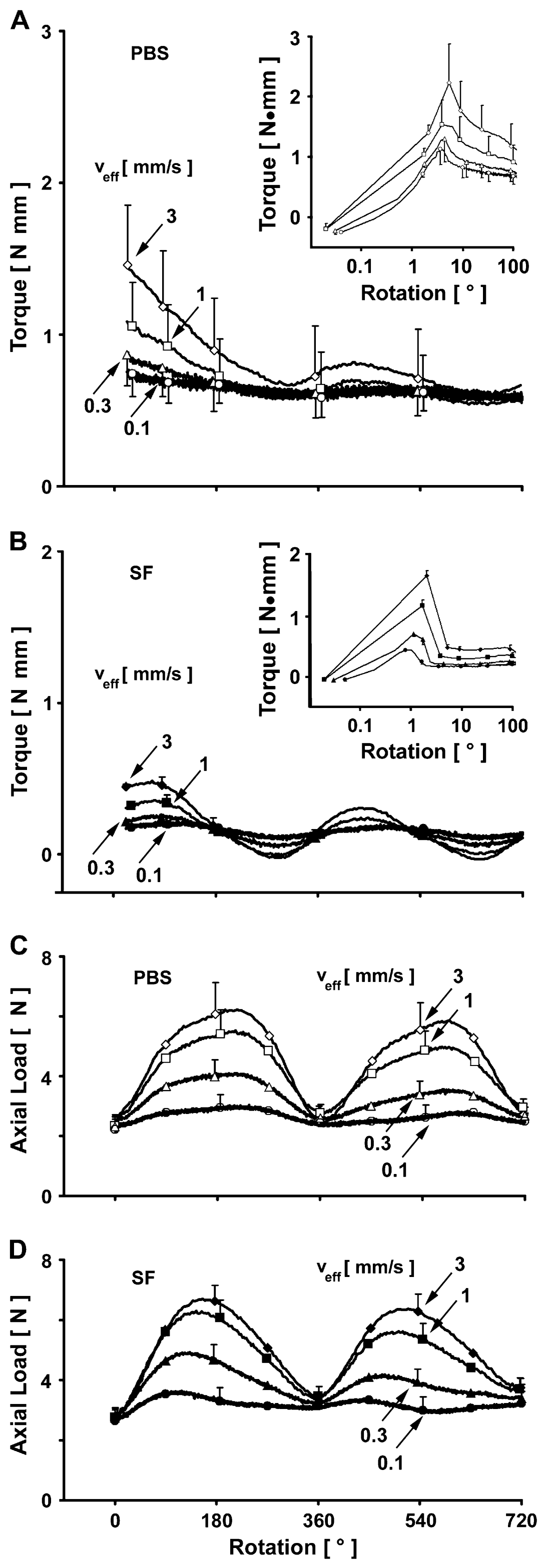

Fig. 5. Torque (A, B with log scale insets to show values at small rotation angles) and axial load (C and D) measurements vs rotation in test baths of PBS and SF at 18% compression ($1-\Lambda_Z$) after 60 min stress relaxation duration (T_{sr}), at effective sliding velocities (v_{eff}) of 3, 1, 0.3, and 0.1 mm/s with a 120 s pre-sliding duration (T_{ps}). Mean ± S.E.M., $n = 4$.

$95 \pm 10\%$ (mean ± SD). The $|N|$ was cyclical during the 2 test revolutions, peaking at approximately 180° and 540°, as noted above [Fig. 3(C,D)]. The respective σ_{peak} values attained in PBS and SF ranged from 0.23 ± 0.02 to 0.11 ± 0.01 MPa and 0.31 ± 0.03 to 0.14 ± 0.01 MPa (for $v_{eff} = 3$–0.1 mm/s) at $1-\Lambda_Z = 12\%$, 0.24 ± 0.02 to 0.13 ± 0.01 MPa and 0.33 ± 0.04 to 0.16 ± 0.02 MPa at $1-\Lambda_Z = 18\%$, and 0.26 ± 0.02 to 0.14 ± 0.02 MPa and 0.36 ± 0.05 to 0.18 ± 0.02 MPa at $1-\Lambda_Z = 24\%$. The respective σ_{eq} values attained in PBS and SF were 0.07 ± 0.01 MPa and 0.07 ± 0.01 MPa at $1-\Lambda_Z = 12\%$, 0.09 ± 0.01 MPa and 0.11 ± 0.01 MPa at $1-\Lambda_Z = 18\%$, and 0.11 ± 0.02 MPa and 0.14 ± 0.02 MPa at $1-\Lambda_Z = 24\%$. Thus, after initial fluid depressurization, $|\tau|$ transients dissipated by the second test revolution, and $|N|$ measurements were generally unaffected by the test lubricant at the various $1-\Lambda_Z$ and v_{eff}.

Friction was modulated by test lubricant, $1-\Lambda_Z$, and v_{eff} (Fig. 6). $\mu_{static,N_{eq}}$ varied with test lubricant ($P < 0.05$), $1-\Lambda_Z$ ($P < 0.05$), and v_{eff} ($P < 0.001$), with an interaction effect between $1-\Lambda_Z$ and v_{eff} ($P < 0.001$) [Fig. 6(A)]. For tests in PBS, $\mu_{static,N_{eq}}$ varied with v_{eff} ($P < 0.001$) and an interaction between $1-\Lambda_Z$ and v_{eff} ($P < 0.05$). For tests in SF, $\mu_{static,N_{eq}}$ varied with $1-\Lambda_Z$, v_{eff} (both $P < 0.001$), and an interaction effect ($P < 0.05$). Values of $\mu_{static,N_{eq}}$ were greater when samples were tested in PBS than when samples were tested in SF, and increased with v_{eff}, ranging from 0.21 to 0.41 in PBS, and 0.074 to 0.28 in SF, at $1-\Lambda_Z = 18\%$. Conversely, $\mu_{static,N_{eq}}$ decreased with $1-\Lambda_Z$ at every v_{eff}, ranging from 0.23 to 0.28 and 0.10 to 0.16 in PBS and SF, respectively, at $v_{eff} = 0.3$ mm/s. This variation with increasing $1-\Lambda_Z$ was attributable to an increase in peak $|\tau|$ that was relatively small compared to the increase in $|N_{eq}|$.

$\langle\mu_{kinetic}\rangle$ varied markedly with test lubricant (being higher in PBS than SF, $P < 0.05$) and slightly with $1-\Lambda_Z$ ($P < 0.05$) but not v_{eff} ($P = 0.16$), with an interaction effect between test lubricant and $1-\Lambda_Z$ ($P < 0.01$) [Fig. 6(B)]. In PBS, $\langle\mu_{kinetic}\rangle$ varied with $1-\Lambda_Z$ ($P < 0.05$), increasing from 0.043 to 0.079 at 3 mm/s, and tended to decrease with v_{eff}. In SF, $\langle\mu_{kinetic}\rangle$ varied with v_{eff} ($P < 0.01$), remaining steady at 0.014 at all $1-\Lambda_Z$ and the lower $v_{eff} = 0.1$–1 mm/s. $\langle\mu_{kinetic,N_{eq}}\rangle$ varied with test lubricant ($P < 0.05$) but not significantly with $1-\Lambda_Z$ ($P = 0.28$) or v_{eff} ($P = 0.56$), with interaction effects between test lubricant and $1-\Lambda_Z$ ($P < 0.001$), $1-\Lambda_Z$ and v_{eff} ($P < 0.01$), and test lubricant, $1-\Lambda_Z$ and v_{eff} ($P < 0.001$) [Fig. 6(C)]. Specifically, in PBS, $\langle\mu_{kinetic,N_{eq}}\rangle$ varied with $1-\Lambda_Z$ ($P < 0.01$) and an interaction between $1-\Lambda_Z$ and v_{eff} ($P < 0.001$); in SF, $\langle\mu_{kinetic,N_{eq}}\rangle$ varied with $1-\Lambda_Z$ ($P < 0.05$) and v_{eff} ($P < 0.01$). In PBS, $\langle\mu_{kinetic,N_{eq}}\rangle$ was greater than in SF, increased with $1-\Lambda_Z$ only at the larger v_{eff}, ranging from 0.080 to 0.13 at 3 mm/s, and remained steady at 0.090 at all $1-\Lambda_Z$ and the lower $v_{eff} = 0.1$–1 mm/s. Similarly in SF, $\langle\mu_{kinetic,N_{eq}}\rangle$ remained steady, at all $1-\Lambda_Z$ and the lower $v_{eff} = 0.1$–1 mm/s, at 0.020. Friction coefficients calculated at the first $v_{eff} = 3$ mm/s were reproduced with the second $v_{eff} = 3$ mm/s, reaching values of $100 \pm 8\%$, $92 \pm 7\%$, $100 \pm 10\%$, and $111 \pm 13\%$ (mean ± SD) for μ_{static}, $\mu_{static,N_{eq}}$, $\langle\mu_{kinetic}\rangle$, and $\langle\mu_{kinetic,N_{eq}}\rangle$, respectively. Therefore, μ_{static}, $\mu_{static,N_{eq}}$, $\langle\mu_{kinetic}\rangle$, and $\langle\mu_{kinetic,N_{eq}}\rangle$ were generally unaffected by the sequence of v_{eff} tested.

EFFECT OF PRE-SLIDING DURATION

The $|\tau|$ [Fig. 7(A,B)] and $|N|$ [Fig. 7(C,D)] during the 2 test revolutions varied with T_{ps}. In both the PBS and SF test lubricants, $|\tau|$ and $|N|$ increased qualitatively with T_{ps}. $|\tau|$ was

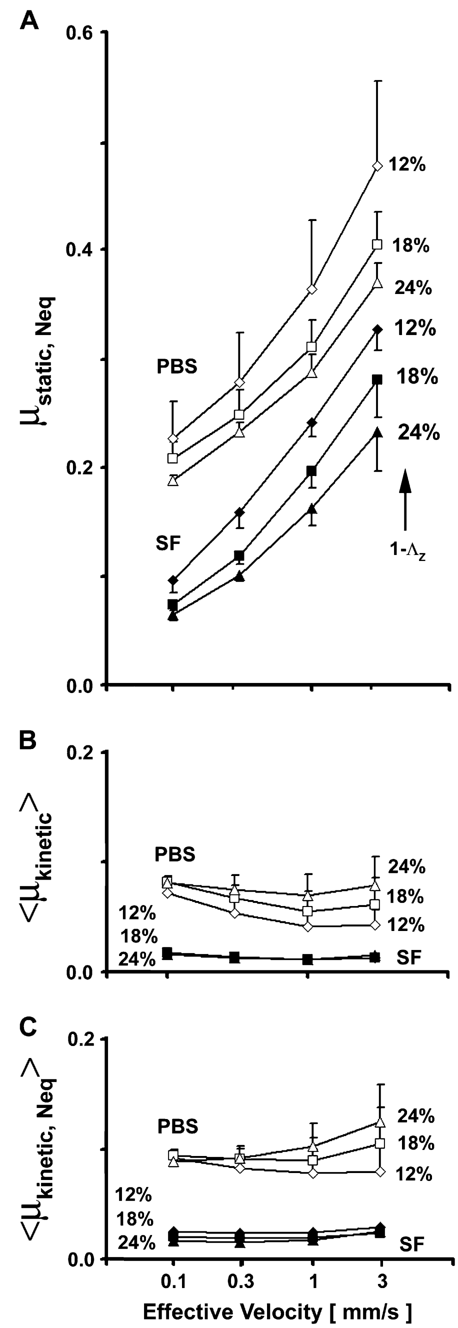

Fig. 6. Static, $\mu_{\text{static},N_{\text{eq}}}$ (A), and kinetic, $\langle\mu_{\text{kinetic}}\rangle$ (B), $\langle\mu_{\text{kinetic},N_{\text{eq}}}\rangle$ (C) friction coefficients in PBS and SF at 12%, 18%, and 24% compression ($1-\Lambda_Z$) after 60 min stress relaxation duration (T_{sr}), at effective sliding velocities (v_{eff}) of 3, 1, 0.3, and 0.1 mm/s with a 120 s pre-sliding duration (T_{ps}). Mean $\pm$ S.E.M., $n=4$.

greater in PBS than SF, while $|N|$ was similar in PBS and SF. Consistent with the data above [Figs. 3(A,B) and 5(A,B)], the peak $|\tau|$ [see insets of Fig. 7(A,B)], dissipated to an approximately steady-state value by 360°. Also consistent with the data above [Figs. 3(C,D) and 5(C,D)], the $|N|$ was cyclical during the 2 test revolutions, peaking at approximately 180° and 540°. The respective σ_{peak} values attained at $1-\Lambda_Z=18\%$ in PBS and SF ranged (for $T_{\text{ps}}=3600-1.2$ s) from 0.36 ± 0.04 to 0.22 ± 0.04 MPa

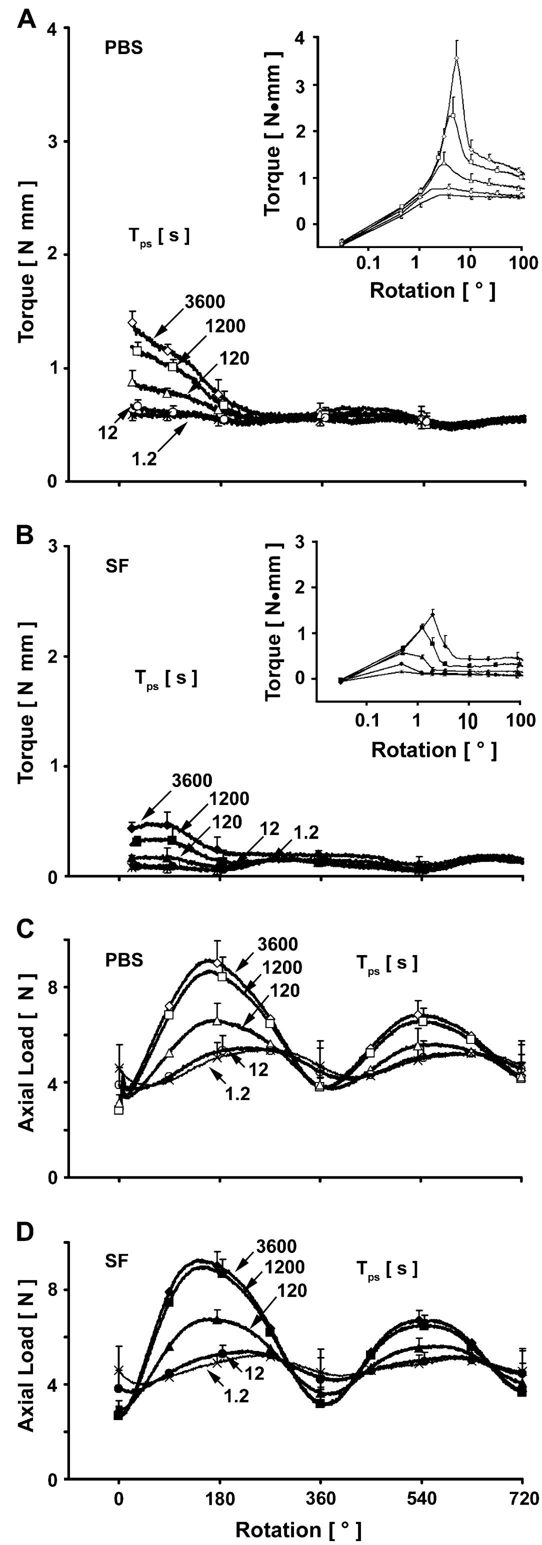

Fig. 7. Torque (A, B with log scale insets to show values at small rotation angles) and axial load (C and D) measurements vs rotation in test baths of PBS and SF at 18% compression ($1-\Lambda_Z$) after 60 min stress relaxation duration (T_{sr}), at an effective sliding velocity (v_{eff}) of 0.3 mm/s with a 3600, 1200, 120, 12, and 1.2 s pre-sliding duration (T_{ps}). Mean $\pm$ S.E.M., $n=4$.

and 0.40 ± 0.02 to 0.24 ± 0.03 MPa. The σ_{eq} values attained at $1-\Lambda_Z = 18\%$ in PBS and SF were both 0.13 ± 0.01 MPa.

Friction was modulated by test lubricant and T_{ps} (Fig. 8). $\mu_{static,N_{eq}}$ varied with test lubricant ($P<0.01$) and T_{ps} ($P<0.001$), with an interaction effect ($P<0.001$) [Fig. 8(A)]. Values of $\mu_{static,N_{eq}}$ were greater in PBS than SF, and increased with T_{ps}, ranging from 0.091 to 0.43 in PBS, and 0.021 to 0.19 in SF. $\langle\mu_{kinetic}\rangle$ varied with test lubricant ($P<0.01$) but not T_{ps} ($P=0.87$), with no interaction effect ($P=0.37$) [Fig. 8(B)]. $\langle\mu_{kinetic}\rangle$ in PBS, 0.054, was greater than that in SF, 0.012. $\langle\mu_{kinetic,N_{eq}}\rangle$ varied with test lubricant ($P<0.001$) and T_{ps} ($P<0.05$) with no interaction effect ($P=0.91$) [Fig. 8(C)]. Similar to $\langle\mu_{kinetic}\rangle$, values of $\langle\mu_{kinetic,N_{eq}}\rangle$ were greater in PBS than SF, and increased slightly with T_{ps}, ranging from 0.077 to 0.082 (mean = 0.079) in PBS, and 0.017 to 0.023 (mean = 0.019) in SF. In both PBS and SF, $\mu_{static,N_{eq}}$ appeared to approach $\langle\mu_{kinetic}\rangle$, and $\langle\mu_{kinetic,N_{eq}}\rangle$, asymptotically as $T_{ps} \to 0$.

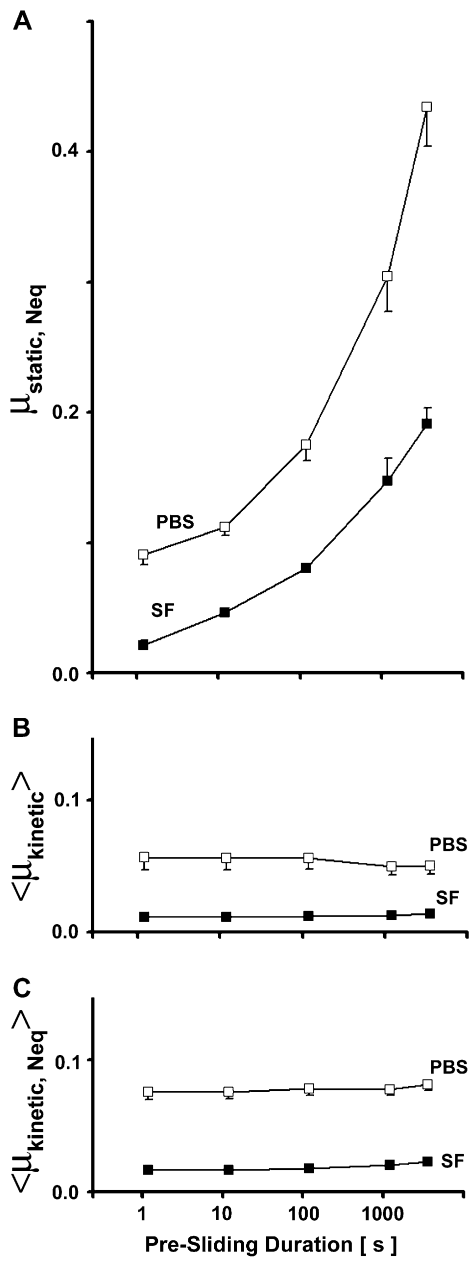

Fig. 8. Static, $\mu_{static,N_{eq}}$ (A), and kinetic, $\langle\mu_{kinetic}\rangle$ (B), $\langle\mu_{kinetic,N_{eq}}\rangle$ (C) friction coefficients in PBS and SF at 18% compression ($1-\Lambda_Z$) after 60 min stress relaxation duration (T_{sr}), at an effective sliding velocity (v_{eff}) of 0.3 mm/s with a 3600, 1200, 120, 12, and 1.2 s pre-sliding duration (T_{ps}). Mean ± S.E.M., $n=4$.

ROLE OF FLUID DEPRESSURIZATION DURING ROTATION

$|N|$ exhibited transient increases during compression and torsion, that diminished subsequently when motion was halted. During compression, $|N|$ increased to a peak (data not shown), and then relaxed [Fig. 9(A)] with a time constant ($t_{1/2}$) of 27 ± 1 s, achieving an N_{eq} of 3.2 ± 0.2 N. During subsequent torsion at the relatively fast v_{eff} of 3 mm/s [Fig. 9(B)], $|N|$ was cyclical and attained maxima at approximately 180°, 540°, and 900° and minima of approximately the initial value at 360° and 720°. Consistent with the findings noted above, just after the start of rotation, $|\tau|$ and thus μ, peaked [see insets of Fig. 9(C,D)], and then diminished to values that varied periodically but were approximately at a steady-state by the second revolution (360–720°). Also consistent with the above findings, $\mu_{static} = 0.27 \pm 0.06$ [shown in Fig. 9(E) inset] was similar to $\mu_{static,N_{eq}} = 0.33 \pm 0.08$ (since $|N|$ immediately after the start of rotation was essentially identical to $|N_{eq}|$), and $\langle\mu_{kinetic}\rangle = 0.025 \pm 0.003$ was less than $\langle\mu_{kinetic,N_{eq}}\rangle = 0.057 \pm 0.010$ (since $|N|$ during rotation from 360° to 720° was greater than $|N_{eq}|$). Then, from the maxima in $|N|$ at 900°, $|N|$ relaxed [Fig. 9(E)] with a time constant ($t_{1/2}$) of 17 ± 1 s, achieving an N_{eq} of 3.0 ± 0.2 N. The normalized time dependence of relaxation [Fig. 9(E), right axis] appeared similar qualitatively to the time-dependent relaxation after the initial ramp compression [Fig. 9(A)].

Discussion

The results described here indicate the annulus-on-disk rotational test configuration may be useful for elucidating boundary lubrication at an articular cartilage-on-cartilage interface. At $v_{eff} = 0.3$ mm/s and $1-\Lambda_Z = 18\%$, μ_{static} and $\langle\mu_{kinetic}\rangle$ varied with T_{sr} in PBS, increasing to peak and approximately steady values of 0.25 and 0.096, respectively. In SF, μ_{static} remained relatively constant at 0.11, while $\langle\mu_{kinetic}\rangle$ varied with T_{sr}, increasing to a peak value of 0.035. After $T_{sr} = 60$ min and initial fluid depressurization, in both PBS and SF, $\mu_{static,N_{eq}}$ was approximately equal to μ_{static} (Fig. 4). Also, at $T_{sr} = 60$ min, slow v_{eff} (0.1, 0.3 and 1 mm/s), and a range of compression levels ($1-\Lambda_Z =$ 18% and 24%), $\langle\mu_{kinetic,N_{eq}}\rangle$ was steady at 0.093 in PBS and 0.018 in SF (Fig. 6). At various T_{ps} (1–3600 s) between the initial fluid depressurization ($T_{sr} = 60$ min) and start of torsion, with $v_{eff} = 0.3$ mm/s and $1-\Lambda_Z = 18\%$, $\langle\mu_{kinetic}\rangle$ and $\langle\mu_{kinetic,N_{eq}}\rangle$ were steady at 0.054 and 0.079 in PBS, and lower at 0.012 and 0.019 in SF, respectively, while $\mu_{static,N_{eq}}$ (which was similar to μ_{static}) increased with T_{ps}, reaching peak values of 0.43 in PBS, and 0.19 in SF (Fig. 8). Collectively these results indicate a boundary lubrication mode is operational at a depressurized articular cartilage-on-cartilage interface with $v_{eff} = 0.3$ mm/s and $1-\Lambda_Z = 18\%$ for the annular geometry used here, since $\langle\mu_{kinetic}\rangle$ was relatively invariant with v_{eff} and $1-\Lambda_Z$, a defining feature of boundary lubrication[15]. The results also indicate SF acts as a boundary lubricant for apposing articular cartilage surfaces.

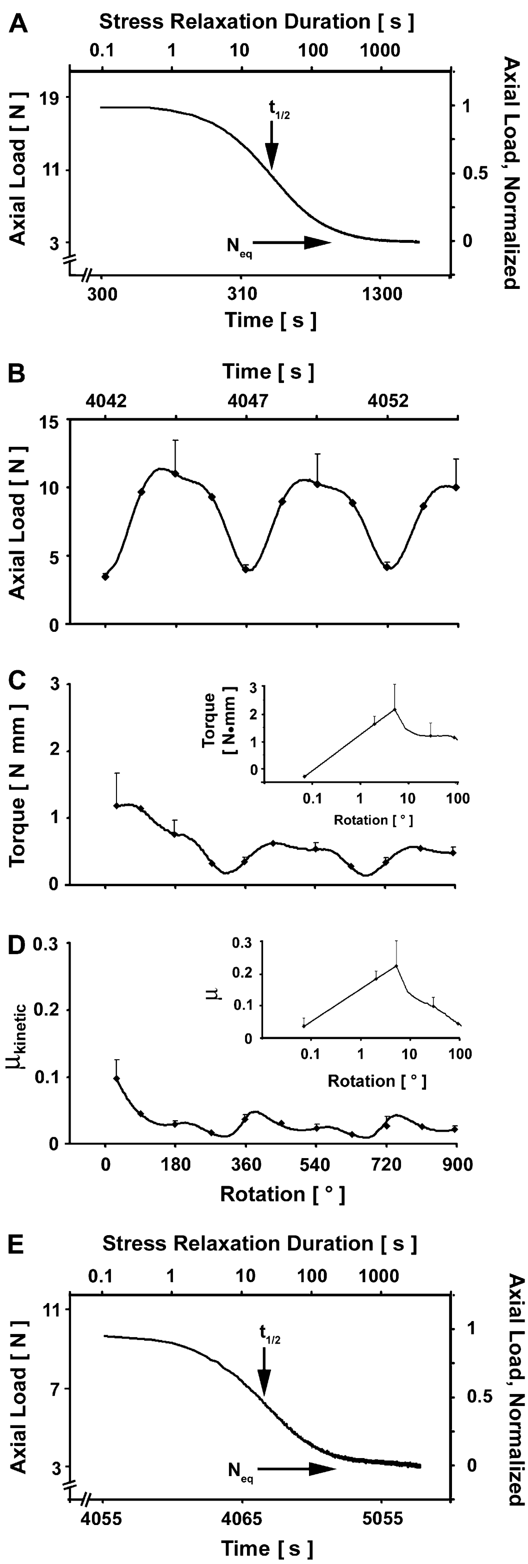

Fig. 9. Axial load measurements following 18% compression ($1-\Lambda_Z$) (A) vs time and stress relaxation duration (T_{sr}). Axial load (B) and torque (with log scale insets) (C) measurements, and resulting friction coefficient μ (with log scale insets) (D), vs rotation at $1-\Lambda_Z=18\%$ after $T_{sr}=60$ min, at an effective sliding velocity (v_{eff}) of 3 mm/s with a 120 s pre-sliding duration (T_{ps}), in a test bath of SF. Axial load measurements following rotation (E) vs time and T_{sr}. Mean ± S.E.M., $n=4$.

The use of fresh osteochondral fragments in the annulus-on-disk rotational test configuration required attention to several experimental and theoretical issues. Samples having a relatively plane cartilage surface, perpendicular to the rotational axis, were verified during test setup by the small axial distance (<0.1 mm, or 4% of the thickness of the apposed articular cartilage) between the initial and final points of contact between the annulus and core (as assessed by $|N|$ during one complete revolution). Cartilage consolidation has been measured to be ~7% *in vivo* by comparison of magnetic resonance imaging (MRI) scans taken before and shortly after various types of exercise[32]. Levels of compression slightly higher than these physiological were used here to ensure full and consistent contact. The resulting tissue surface conformation, due to the depth-varying intrinsic material properties of articular cartilage[33,34], may have circumvented the need for a gimbaled joint, which is desirable when testing synthetic surfaces[35] to avoid the generation of a fluid wedge. The consistency of friction coefficients calculated from tests over a range of compression amplitudes (12–24%) suggests that the values at the 18% levels of $1-\Lambda_Z$ are physiologically relevant. Potential directional effects on τ measurements were accounted for by averaging the + and − test revolutions and resulted in moderately low variability in μ, both within (coefficient of variation (CV) 14–21%) and between animals (CV 19–30%), at $1-\Lambda_z=18\%$, $T_{sr}=60$ min, $v_{eff}=0.3$ mm/s, and $T_{ps}=120$ s. Therefore, with attention to test sample preparation, and subsequent characterization of friction properties, fresh osteochondral samples from non-apposing locations within the synovial joint, can be tested *in vitro* to analyze boundary lubrication at articulating cartilage surfaces.

The cyclical nature of the $|N|$ during rotation (after initial fluid depressurization following axial compression), and the effects of rotation on $|\tau|$ appeared to be explained predominantly by fluid pressurization during rotation, based on experimental and theoretical considerations. Indeed, a similar velocity dependent normal stress was observed when articular cartilage was rotated against a steel surface[19], suggesting that the effect was not due to the fact that both apposed surfaces were articular cartilage. The authors proposed that this effect resulted from steady flow of fluid through the porous permeable solid matrix of cartilage, and possibly from the charged nature of the tissue matrix. In the present study, when rotation was halted, $|N|$ relaxed to $|N_{eq}|$ with a time constant characteristic of fluid depressurization [Fig. 9(A,E)]. Indeed, the extent of fluid pressurization may be represented by the difference between values of σ_{peak} and σ_{eq}. During this time, $|\tau|$ oscillated, but with an average value during the second test revolution that was virtually unaffected (verified by the ratio of $\tau_{360-720°}$ to $\tau_{360°}$ being 95 ± 10% (mean ± SD)). This is further supported by $\langle\mu_{kinetic,N_{eq}}\rangle$ being unaffected by v_{eff} at higher compression [$1-\Lambda_Z=18\%$, used in most experiments, and 24%, Fig. 6(C)], and $\langle\mu_{kinetic}\rangle$ generally decreasing with increasing v_{eff} [Fig. 6(B)] and consistently being less than the $\langle\mu_{kinetic,N_{eq}}\rangle$ in all test protocols and lubricants [Figs. 6 and 8]. Therefore, $\langle\mu_{kinetic,N_{eq}}\rangle$ is an appropriate measure of the frictional response of articular cartilage, minimizing the effects of fluid pressurization, under boundary lubricating conditions, especially for tests at the lower effective sliding velocities.

The results obtained here are consistent with and extend the earlier studies of Davis[25,35] and Malcom and Fung[16,26]. In Davis' studies, bovine SF lubricated planed nasal septal cartilage surfaces better than Gey's balanced salt solution at various compressive loads (0.1–0.3 MPa) and v_{eff} (0.5–2.5 mm/s). A direct comparison of μ values is difficult due to the different cartilaginous tissue tested, and the duration allowed to reach equilibrium, nonetheless, $\mu \sim 0.025$ in SF at $v_{\mathrm{eff}} = 1$ mm/s is similar to the $\langle \mu_{\mathrm{kinetic},N_{\mathrm{eq}}} \rangle = 0.022$ reported here [Fig. 6(C)]. Although the effect of fluid pressurization was not characterized, the maintenance of SF's lubricating ability after hyaluronidase treatment implied a boundary mode lubrication was dominant. Davis ultimately reported inconsistencies with repeated testing of the same lubricant and abandoned the use of septal cartilage. This may have resulted from planed septal cartilage surfaces lacking specialized properties of articular cartilage and articular cartilage surfaces, where interactions with lubricant molecules in SF may occur. The relatively low modulus near the surface of articular cartilage may have facilitated the conformation of apposing surfaces[33]. In the studies of Malcom and Fung, SF also lubricated better than PBS under various static loads (0.05–5 MPa) at $v_{\mathrm{eff}} = \sim 4$ mm/s after creep. The time dependence of $\langle \mu_{\mathrm{kinetic}} \rangle$ at an articular cartilage-on-cartilage interface during creep, rather than stress relaxation (Fig. 4), was demonstrated. Malcom and Fung reported $\langle \mu_{\mathrm{kinetic}} \rangle = 0.005 \pm 0.001$ in SF vs $\langle \mu_{\mathrm{kinetic}} \rangle = 0.010 \pm 0.002$ in PBS (mean $\pm$ SD) at ~ 0.1 MPa, with a relative insensitivity of shear friction and therefore $\langle \mu_{\mathrm{kinetic}} \rangle$, to shearing velocity ($v_{\mathrm{eff}}$), over the range presented here (Fig. 6). This supports the assertion that the annulus-on-disk rotational configuration is amenable to boundary lubrication of articular cartilage as well. The effect of T_{ps} on μ_{static}, but not $\langle \mu_{\mathrm{kinetic}} \rangle$, was also observed, as in the present study (Fig. 8), with μ_{static} ranging from ~ 0.01 to 0.1 in PBS, and 0.005 to 0.015 in SF, for $T_{\mathrm{ps}} = 0$–8 min at $v_{\mathrm{eff}} = \sim 4$ mm/s. Direct comparison of μ values is again difficult due to differences in loading protocols, and the duration of rotation and fluid depressurization. The values for $\langle \mu_{\mathrm{kinetic}} \rangle$ reported by Malcom and Fung are approximately 10-fold less than those reported here at similar test parameters, which may be due to continuous rotation during the relatively short time allowed for creep (12 min), since the shear force was shown to increase with time and continuous rotation may 'align' boundary lubricating molecules at the surface. Therefore, the lubrication test configuration developed here is a modified version of that developed by Davis and by Malcom and Fung, with expanded test protocols and characterization.

The effect of fluid pressurization within cartilage on μ is consistent with and extends several studies as well. Wang and Ateshian[19] observed that the normal stress under a prescribed infinitesimal compressive strain increased with increasing sliding velocity, similar to that found in the present study (Fig. 5, and in pilot studies with an articular cartilage–polysulfone interface, data not shown), using a plate on plate geometry within a rotational friction apparatus. Krishnan *et al.*[17] demonstrated a negative correlation between the temporal variations of the effective friction coefficient (μ_{Eff}) of cartilage with the interstitial load support using a reciprocating friction apparatus ($v = 1$ mm/s) articulating cartilage against glass. Using previously frozen samples, PBS as a test lubricant, and a prescribed load of 4.5 N ($\sigma = 0.16$ MPa for the sample geometry), $\mu_{\mathrm{Eff}} = \sim 0.25$ was reported after fluid depressurization, more than double compared to the values reported for the corresponding $\langle \mu_{\mathrm{kinetic}} \rangle$ and $\langle \mu_{\mathrm{kinetic},N_{\mathrm{eq}}} \rangle$ at $v_{\mathrm{eff}} = 1$ mm/s, and $1 - \Lambda_Z = 24\%$ [Fig. 6(B,C)]. However, in a subsequent study using fresh cartilage samples and the same friction apparatus to assess the role of the superficial zone of articular cartilage when articulated against glass, lower values for $\mu_{\mathrm{Eff}} = \sim 0.15$ after fluid depressurization were reported[36], which are in agreement with values reported for fresh samples here (μ was not determined in SF in either of these studies). The diminished effect of T_{sr}, and hence fluid depressurization, on the frictional properties of articular cartilage in SF compared to PBS (Fig. 4) may be indicative of lubricant molecules interacting with the articular cartilage surface and modulating the frictional response. The time dependence of the friction properties of cartilage has also been observed in a reciprocating motion friction test using cartilage-on-metal contacts, although the absolute values of μ were much greater[7].

The boundary lubricating ability of SF demonstrated here is consistent with several other studies using various friction apparatuses and test surfaces. Jones originally measured μ of cartilage against cartilage, at very slow rubbing speeds using a horse stifle joint, to be 0.02 in SF[37]. Charnley repeated Jones' experiments using a similar apparatus, and found very low $\mu = 0.005$–0.024[38]. However, other studies of that era indicated that SF had very little lubricating ability between non-cartilaginous surfaces[37,39]. Linn[15] reported similarly low levels of $\mu = 0.004$ using bovine SF in excised dog ankle joints using an arthrotripsometer. Using a gimbaled annulus-on-disk rotational test configuration, Davis *et al.* showed bovine SF enhanced boundary lubrication between specific synthetic surfaces, latex on glass, resulting in a $\mu = \sim 0.021$[25]. More recently, Jay *et al.* reported healthy bovine and human SF to have a $\mu = 0.019$–0.028[40,41] and $\mu = \sim 0.025$[42], respectively, under boundary lubricating conditions. Even though a wide range of μ values are reported in tests using intact joints, likely due to the complex articular cartilage-on-cartilage interaction, the historical values obtained by Jones in the stifle joint and the upper limit of Charnley's are consistent with those obtained here $\mu \sim 0.02$ (Fig. 6). It remains unclear if the physiological molecular structure, and interactions, of boundary lubricants between articular cartilage surfaces are recapitulated with asymmetric synthetic test surfaces, such as latex and glass[25]. Nevertheless, the agreement with μ values obtained here using articular surfaces in a similar test configuration suggests specific synthetic surfaces are useful for studying putative physiological boundary lubricants as well.

The dependency of $\mu_{\mathrm{static},N_{\mathrm{eq}}}$ on T_{ps}, and other test parameters, is consistent with and extends studies by Forster and Fisher[6]. They demonstrated the stationary loading time dependence of the start-up friction coefficient, with μ values in bovine SF at an articular cartilage-on-cartilage interface ranging from ~ 0.02 to 0.25 with increasing loading time from 5 s to 45 min under a mixed lubrication regime ($\sigma = 0.5$–4 MPa and $v = 4$ mm/s) using a sliding friction machine. Although fluid pressure effects may have been present immediately after start-up due to the linear nature of the system with the cartilage plug sliding along a previously unloaded and therefore fully hydrated cartilage surface, the start-up friction coefficient values are consistent with $\mu_{\mathrm{static},N_{\mathrm{eq}}}$ found here at a slower $v_{\mathrm{eff}} = 0.3$ mm/s ranging from 0.02 to 0.19 [Fig. 8(A)]. Interestingly, they also demonstrated the ability of bovine SF to reduce start-up friction at a cartilage-on-cartilage interface was lost at a cartilage-on-metal interface. Finally, the inverse dependence of $\mu_{\mathrm{static},N_{\mathrm{eq}}}$ on $1 - \Lambda_Z$ in both lubricants [Fig. 6(A)] may be indicative of restrained surface tissue shear at start-up, and potentially chondrocyte protection from wear and mechanical disturbances *in vivo*.

The paradigm of several operational lubrication modes during cartilage articulation within the synovial joint[5] has long been generally accepted. Recently, the natural lubricant constituents in SF such as proteins, lipids, and hyaluronic acid were proposed to act synergistically in the synovial joint through adaptive multimode lubrication[43]. Dowson stated that a full appreciation of the tribological performance of joints can be achieved only when it is known whether the mode of lubrication is fluid film, boundary or mixed, and, that previous attempts to ascribe a single mode of lubrication to synovial joints have undoubtedly delayed the emergence of a satisfactory overall picture of the performance of nature's bearing[11]. Although the various friction properties of articular cartilage characterized in this study have been previously demonstrated, the wide range of reported μ values indicates the need for careful characterization of the test setup, sample surface, preparation and storage, and resulting measurements in control type lubricants to identify the operating lubrication mode. Only then can quantitative, mechanistic statements be made about the boundary lubricating properties of cartilage within synovial joints. Therefore, this test configuration, particularly with parameters of $v_{\mathrm{eff}} = 0.3$ mm/s and $1 - \Lambda_Z = 18\%$, after fluid depressurization, is useful for defining the lubrication properties of putative fluid lubricants; it may also allow elucidation of the components of SF that function, independently, additively, or synergistically, as boundary lubricants[15,29,44–47] through potentially specific interactions with native articular cartilage surfaces.

Acknowledgments

This work was supported by NIH and NSF.

References

1. Stockwell RA. Biology of Cartilage Cells. New York: Cambridge University Press 1979, 316 pp.
2. Seedhom BB, Wallbridge NC. Walking activities and wear of prostheses. Ann Rheum Dis 1985;44:838–43.
3. Buckwalter JA, Mankin HJ. Articular cartilage. Part II: degeneration and osteoarthrosis, repair, regeneration, and transplantation. J Bone Joint Surg Am 1997;79-A: 612–32.
4. Ateshian GA, Mow VC. Friction, lubrication, and wear of articular cartilage and diarthrodial joints. In: Mow VC, Huiskes R, Eds. Basic Orthopaedic Biomechanics and Mechano-Biology. Philadelphia: Lippincott Williams & Wilkins 2005:447–94.
5. Wright V, Dowson D. Lubrication and cartilage. J Anat 1976;121:107–18.
6. Forster H, Fisher J. The influence of loading time and lubricant on the friction of articular cartilage. Proc Inst Mech Eng [H] 1996;210:109–19.
7. Forster H, Fisher J. The influence of continuous sliding and subsequent surface wear on the friction of articular cartilage. Proc Inst Mech Eng [H] 1999;213: 329–45.
8. McCutchen CW. Boundary lubrication by synovial fluid: demonstration and possible osmotic explanation. Fed Proc 1966;25:1061–8.
9. Morrell KC, Hodge WA, Krebs DE, Mann RW. Corroboration of *in vivo* cartilage pressures with implications for synovial joint tribology and osteoarthritis causation. Proc Natl Acad Sci U S A 2005;102:14819–24.
10. Meyer E, Overney RM, Dransfeld K, Gyalog T. Nanoscience: Friction and Rheology on the Nanometer Scale. River Edge, New Jersey: World Scientific Publishing Co. Pte. Ltd 2002, 373 pp.
11. Dowson D. New joints for the millennium: wear control in total replacement hip joints. Proc Inst Mech Eng [H] 2001;215:335–58.
12. Murakami T, Sawae Y, Ihara M. Protective mechanism of articular cartilage to severe loading: roles of lubricants, cartilage surface layer, extracellular matrix and chondrocyte. JSME Int J Series C-Mechanical Systems Machine Elements & Manufacturing 2003; 46:594–603.
13. Meachim G. Light microscopy of Indian ink preparations of fibrillated cartilage. Ann Rheum Dis 1972;31: 457–64.
14. Linn FC. Lubrication of animal joints. I. The arthrotripsometer. J Bone Joint Surg Am 1967;49-A:1079–98.
15. Linn FC. Lubrication of animal joints. II. The mechanism. J Biomech 1968;1:193–205.
16. Malcom LL. An experimental investigation of the frictional and deformational responses of articular cartilage interfaces to static and dynamic loading. Ph.D. thesis, University of California, San Diego, 1976.
17. Krishnan R, Kopacz M, Ateshian GA. Experimental verification of the role of interstitial fluid pressurization in cartilage lubrication. J Orthop Res 2004;22:565–70.
18. Park S, Costa KD, Ateshian GA. Microscale frictional response of bovine articular cartilage from atomic force microscopy. J Biomech 2004;37:1679–87.
19. Wang H, Ateshian GA. The normal stress effect and equilibrium friction coefficient of articular cartilage under steady frictional shear. J Biomech 1997;30: 771–6.
20. Benz M, Chen N, Jay G, Israelachvili J. Static forces, structure and flow properties of complex fluids in highly confined geometries. Ann Biomed Eng 2005; 33:39–51.
21. Kwan MK, Lai WM, Mow VC. Fundamentals of fluid transport through cartilage in compression. Ann Biomed Eng 1984;12:537–58.
22. Ateshian GA, Wang H. A theoretical solution for the frictionless rolling contact of cylindrical biphasic articular cartilage layers. J Biomech 1995;28:1341–55.
23. Ateshian GA, Lai WM, Zhu WB, Mow VC. An asymptotic solution for the contact of two biphasic cartilage layers. J Biomech 1994;27:1347–60.
24. Bowden FP, Tabor D. The Friction and Lubrication of Solids. New York: Oxford University Press 1950, 384 pp.
25. Davis WHJ, Lee SL, Sokoloff L. A proposed model of boundary lubrication by synovial fluid: structure of boundary water. J Biomech Eng 1979;101:185–92.
26. Fung YC. Biomechanics: Mechanical Properties of Living Tissues. New York: Springer-Verlag 1981.
27. Williamson AK, Chen AC, Sah RL. Compressive properties and function–composition relationships of developing bovine articular cartilage. J Orthop Res 2001;19:1113–21.
28. Kurtis MS, Tu BP, Gaya OA, Mollenhauer J, Knudson W, Loeser RF, *et al.* Mechanisms of chondrocyte adhesion to cartilage: role of β1 integrins, CD44, and annexin V. J Orthop Res 2001;19: 1122–30.
29. Jay GD, Harris DA, Cha C-J. Boundary lubrication by lubricin is mediated by O-linked β(1–3)Gal–GalNAc oligosaccharides. Glycoconj J 2001;18:807–15.
30. Frank EH, Grodzinsky AJ. Cartilage electromechanics-II. A continuum model of cartilage electrokinetics and

correlation with experiments. J Biomech 1987;20: 629–39.
31. Mow VC, Kuei SC, Lai WM, Armstrong CG. Biphasic creep and stress relaxation of articular cartilage in compression: theory and experiment. J Biomech Eng 1980;102:73–84.
32. Eckstein F, Lemberger B, Gratzke C, Hudelmaier M, Glaser C, Englmeier KH, *et al*. *In vivo* cartilage deformation after different types of activity and its dependence on physical training status. Ann Rheum Dis 2005;64:291–5.
33. Schinagl RM, Gurskis D, Chen AC, Sah RL. Depth-dependent confined compression modulus of full-thickness bovine articular cartilage. J Orthop Res 1997;15:499–506.
34. Chen AC, Bae WC, Schinagl RM, Sah RL. Depth- and strain-dependent mechanical and electromechanical properties of full-thickness bovine articular cartilage in confined compression. J Biomech 2001; 34:1–12.
35. Davis WHJ, Lee SL, Sokoloff L. Boundary lubricating ability of synovial fluid in degenerative joint disease. Arthritis Rheum 1978;21:754–60.
36. Krishnan R, Caligaris M, Mauck RL, Hung CT, Costa KD, Ateshian GA. Removal of the superficial zone of bovine articular cartilage does not increase its frictional coefficient. Osteoarthritis Cartilage 2004; 12:947–55.
37. Jones ES. Joint lubrication. Lancet 1934;223:1426–7.
38. Charnley J. Lubrication of animal joints. Proc Symp Biomech 1959;12–22.
39. Tanner RI, Edwards FJ. The lubrication properties of synovial fluid, in Appendix 5 of Charnley (1959). 1959.
40. Jay GD, Haberstroh K, Cha C-J. Comparison of the boundary-lubricating ability of bovine synovial fluid, lubricin, and Healon. J Biomed Mater Res 1998;40: 414–8.
41. Jay GD, Cha D-J. The effect of phospholipase digestion upon the boundary lubricating activity of synovial fluid. J Rheumatol 1999;26:2454–7.
42. Jay GD, Marcelino J, Al-mayouf S, Laxer R, Rhee DK, Cha CJ, *et al*. Synovial fluid from patients with camptodactyl-arthropathy-coxa vara-pericarditis (CACP) lacks boundary lubricating ability. Trans Orthop Res Soc 2003;28:134.
43. Murakami T, Higaki H, Sawae Y, Ohtsuki N, Moriyama S, Nakanishi Y. Adaptive and multimode lubrication in natural synovial joints and artificial joints. Proc Inst Mech Eng [H] 1998;212:23–35.
44. Swann DA, Radin EL. The molecular basis of articular lubrication. J Biol Chem 1972;247:8069–73.
45. Schwarz IM, Hills BA. Surface-active phospholipids as the lubricating component of lubricin. Br J Rheumatol 1998;37:21–6.
46. Hills BA, Monds MK. Enzymatic identification of the load-bearing boundary lubricant in the joint. Br J Rheumatol 1998;37:137–42.
47. Schmid T, Soloveychik V, Kuettner K, Schumacher B. Superficial zone protein (SZP) from human cartilage has lubrication activity. Trans Orthop Res Soc 2001; 26:178.